ELSEVIER

Catalysis Today 70 (2001) 169–181

CATALYSIS TODAY

www.elsevier.com/locate/cattod

Oxidative properties of niobium-containing mesoporous silica catalysts

Maria Ziolek*, Izabela Sobczak, Anna Lewandowska, Izabela Nowak, Piotr Decyk, Monika Renn, Beata Jankowska

Faculty of Chemistry, A. Mickiewicz University, Grunwaldzka 6, 60-780 Poznan, Poland

Abstract

Oxidative properties of MCM-41 molecular sieves containing niobium in the framework or/and in the extra framework positions were studied by means of H_2-TPR, FTIR + NO, ESR techniques and were tested in the oxidation of dibutyl sulphide with hydrogen peroxide. The application of various Nb-sources in the synthesis of NbMCM-41 materials allows the estimation of a role of oxalate ions in the generation of active centres. The activity of Nb-containing mesoporous molecular sieves in the oxidation of thioethers with H_2O_2 requires the presence of Nb–O^- species in the framework. The growth of a concentration of niobium (from Si/Nb = 32 to Si/Nb = 16) results in the decrease of the number of active centres due to the release of oxygen during the activation procedure. Niobium species in the extra framework positions of MCM-41 catalysts are not active in the dibutyl sulphide oxidation with H_2O_2 unless they are leached to the solution. Oxidative centres on the catalyst surface cause the formation of nitrite/nitrate species after the adsorption of NO.

Keywords: Niobium-containing MCM-41; H_2-TPR; ESR; NO adsorption — FTIR; Oxidation of thioethers

1. Introduction

The synthesis of redox molecular sieves with large pore diameters and a various chemical composition is in the field of interest of many research groups. It is due to the application of these sieves in the catalytic oxidation widely used in the production of fine chemicals [1–3]. The development in the synthesis of the molecular sieves allows tailoring of them and optimisation of the catalyst–substrate interaction. The most important is a proper choice of metal and oxidant according to the oxidation mechanism involved.

Catalytic oxidations can be divided into three basic categories [2,4]: (i) free-radical autooxidation, (ii) oxidation of coordinated substrates followed by reoxidation of the reduced metal ion, and (iii) catalytic oxygen transfer. The latter is the reaction of an oxygen donor, e.g. H_2O_2, with an organic substrate in the presence of a metal catalyst. The active oxidant in such processes may be an oxometal or peroxometal species depending on the nature of a metal element in the catalyst. However, some elements, such as vanadium, reacts via oxometal or peroxometal intermediates depending on the substrate. In the peroxometal pathway there is no change in the oxidation state of the metal ion during the reaction (metal ion act as a Lewis acid increasing of the oxidising power of the peroxo group). This pathway is heterolytic in nature and requires oxygen donors such as H_2O_2 or RO_2H. Early transition metal ions, like Ti(IV), Mo(VI) and W(VI), exhibit a tendency to the peroxometal pathway. Olefin epoxidation, sulphoxidation, oxidation of various nitrogen compounds, and

* Corresponding author. Tel.: +48-61-829-1243.
E-mail address: ziolek@amu.edu.pl (M. Ziolek).

0920-5861/01/$ – see front matter
PII: S0920-5861(01)00416-3

alcohol oxidation proceed according to this way. In the oxometal pathway, the metal ions — usually late and/or many first-row transition elements (Cr, Mn, Fe) — undergoes a two-electron reduction and is subsequently reoxidised by the oxygen donor (for instance molecular oxygen). In both pathways, it is often difficult to differentiate between a heterolytic, Mars–van Krevelen-type mechanism, and competing homolytic pathways via alkoxy and alkylperoxy radical intermediates. It is probable that niobium-containing catalysts act like vanadium one, i.e. react via oxometal or peroxometal intermediates, depending on the substrate.

The framework substituted titanium silicalite (TS-1), discovered by Enichem scientists in 1983 [4], expanded the application of the heterogeneous catalysts in the liquid phase oxidation. Metal, in the molecular sieves, introduced to the extra framework position by a cation exchange is easily leached during the reaction carried out in a liquid phase. The incorporation of the metal ion into the framework allows the protection from a leaching process. Recently, mesoporous molecular sieves containing various transition metals in the framework were synthesised. Among them niobium silicalite MCM-41 materials were prepared [5–7]. The incorporation of Nb(V) instead of Si(IV) in MCM-41 mesoporous molecular sieves generates an excess positive charge in the framework. In the earlier papers [8,9], we proposed that it is balanced by hydroxyl groups, rather not by non-framework anions because cation exchange properties were found for these materials. The following equation was proposed for the dehydroxylation of NbMCM-41 molecular sieves:

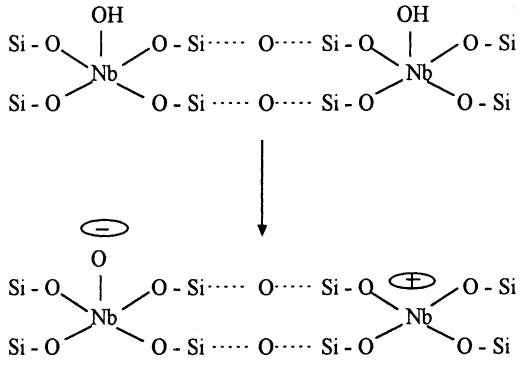

(1)

The presence of Nb–O^- and Nb^+ species was designed on the basis of ESR, NO/FTIR studies [8], and the oxidative properties in catalysis. Formerly, NbMCM-41 materials were prepared from Nb-oxalate used as a niobium source. It is known that oxalate ions can form complexes which play a role of the oxidising centres [10,11].

To avoid the doubts concerning the origin of the active oxygen in NbMCM-41 sieves, the preparation of the materials using various Nb-sources (niobium chloride and niobium ammonium-oxalate complex) was undertaken [12]. In this paper, we present the characterisation of physicochemical properties of the prepared materials by means of FTIR, H_2-TPR, and ESR techniques and their activity in the oxidation of dibutyl sulphide with hydrogen peroxide. Moreover, the materials obtained via niobium-impregnation of MCM-41 and silica were investigated to distinguish between the role of the framework and extra framework niobium species.

2. Experimental

2.1. Catalysts

Niobium was incorporated to the mesoporous molecular sieves of MCM-41 type during the synthesis carried out due to the description presented in [5,6,12]. Three various niobium sources were applied for the synthesis: niobium-oxalate, chloride and ammonium-oxalate complex. Moreover, the impregnation of siliceous MCM-41 and amorphous silica with niobium-oxalate and chloride were conducted. The catalysts used in this work, their compositions, and pore volumes are given in Table 1.

2.2. H_2-TPR

The temperature-programmed reduction (TPR) of the samples was carried out using H_2/Ar (10 vol.%) as reductant (flow rate = 32 $cm^3\,min^{-1}$). The sample of 0.04 g was filled in a quartz tube, treated in a flow of helium at 723 K for 1 h and cooled to the room temperature. Then, it was heated at a rate of 10 K min^{-1} to 1300 K under the reductant mixture. Hydrogen consumption was measured by a thermal conductivity detector in the PulseChemiSorb 2705 (Micromeritics) apparatus.

Table 1
Symbols, composition and physical properties of the catalysts used in this work

Catalyst[a]	Nb-source/preparation	Si/Nb	Total pore volume ($cm^3\ g^{-1}$) (BJH — des.)
MCM-41	–	–	1.19
Nb(O)MCM-41-16	Nb(V) oxalate synthesis	16	1.37
Nb(O)MCM-41-32	Nb(V) oxalate synthesis	32	1.55
Nb(Oc)MCM-41-32	Nb(V) ammonium oxalate complex synthesis	32	1.52
Nb(Cl)MCM-41-32	Nb(V) chloride synthesis	32	1.10
Nb(O)/MCM-41-16	Nb(V) oxalate impregnation	16	0.58
Nb(O)/MCM-41-32	Nb(V) oxalate impregnation	32	0.66
Nb(Cl)/MCM-41-32	Nb(V) chloride impregnation	32	1.04
Nb(O)/SiO_2-32	Nb(V) oxalate impregnation	32	–

[a] The last number denotes the total Si/Nb ratio.

2.3. FTIR measurements

Infrared spectra were recorded with the Vector 22 (Bruker) FTIR spectrometer. The samples were pressed, under low pressure, into thin wafers of ∼10 mg cm^{-2} and placed in the vacuum cell, where they underwent all activation and adsorption treatments. Spectra were registered at the room temperature (RT). The spectrum without any sample ("background spectrum") was scanned and was evidently subtracted from all recorded spectra. Before the measurements, the samples were activated at 723 K under vacuum. The IR spectra of the activated samples were subtracted from those registered after NO adsorption at RT followed by various treatments. The reported spectra are the results of this subtraction. Only the spectra shown in the 850–1000 cm^{-1} region are original without subtraction of the spectrum after activation.

The spectra in the skeletal region (400–1300 cm^{-1}) were also scanned for the samples mixed with KBr (1 mg of sample and 200 mg of KBr).

2.4. ESR study

The ESR measurements were conducted after evacuation of the catalyst at various temperatures (RT to 723 K), and after calcination in the presence of oxygen at 723 K. ESR spectra were recorded at 77 K on a RADIOPAN SE/X 2547 spectrometer. The patterns were obtained at $\nu_{ESR} = 8.9$ GHz. The g-value was calculated according to the commonly used equation: $g = h\nu/\mu_B B$.

2.5. Oxidation of thioeters with hydrogen peroxide

The catalytic reaction between thioethers and hydrogen peroxide was carried out in a glass flask equipped with a magnetic stirrer, a thermocouple, a reflux condenser and a membrane for sampling. A calcinated catalyst of 0.04 g was placed in the flask, where methanol was added. The oxidation was conducted simply by efficiently stirring at first of a mixture of methanol (MeOH) and the catalyst at 303 K. After stirring for ∼1 h, 96% *n*-dibutyl sulphide (*n*-Bu_2S — 2 mmol) was added, followed by the dropwise addition of 31% hydrogen peroxide (2 mmol) to achieve the stoichiometry under Eq. (2),

$$Bu_2S + H_2O_2 \rightarrow Bu_2SO + H_2O \quad (2)$$

The reaction mixtures were analysed each 30 min with Chrom-5 chromatograph equipped with a packed column of Apiezon L (10 wt.%) on Chromosorb W operated at 443 K and a flame ionisation detector (FID). The first analysis was done after 10 min from the beginning of the reaction.

Moreover, the reaction was conducted in the homogeneous phase, i.e. in the methanol solution of niobium-oxalate (the concentration of Nb in the solution was equivalent to that one which could be obtained if the whole niobium from 0.04 g NbMCM-41-16 is leached to the reaction solution).

3. Results

3.1. H_2-TPR

In order to analyse the reducibility of niobium-containing catalysts the temperature-programmed reduction (H_2-TPR) of the samples were performed. Fig. 1 displays the H_2-TPR profiles of various catalysts. In part A, one can compare the profiles of the materials prepared using various niobium sources and applying the Si/Nb ratio in the synthesis = 32. Profiles (a) and (b) exhibit a similar shape which can be divided into two parts: a low temperature (LT) and a high temperature (HT) regions. In the LT range (up to 1000 K) an increasing hydrogen consumption occurs leading to a broad peak covering more than one reduced species, with a maximum at ~870 K (sample a) and 930 K (sample b). In the HT range

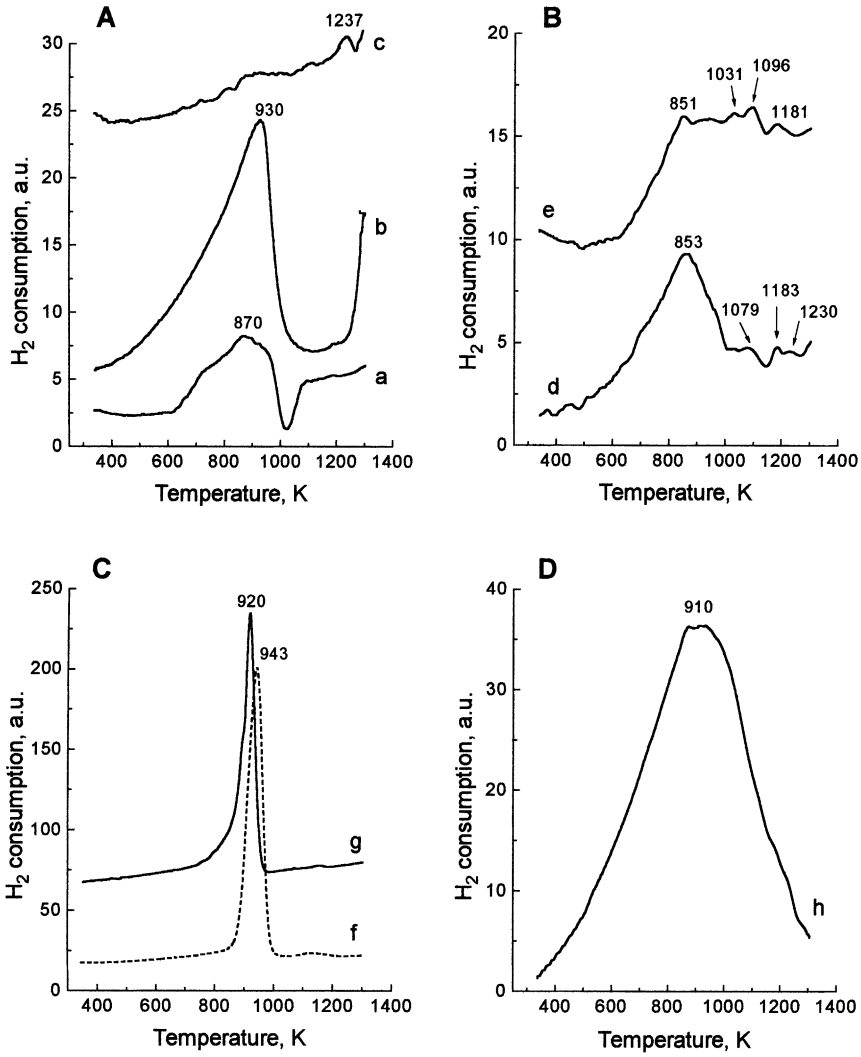

Fig. 1. H_2-TPR profiles of A — NbMCM-41-32 synthesised with various Nb-sources; B — materials with Si/Nb = 16; C — MCM-41 impregnated with various Nb-salts; D — Nb-impregnated silica. The profiles represent the following materials: (a) Nb(O)MCM-41-32; (b) Nb(Cl)MCM-41-32; (c) Nb(Oc) MCM-41-32; (d) Nb(O)MCM-41-16; (e) Nb(O)MCM-41-16 calcined at 723 K in the presence of oxygen; (f) Nb(O)/MCM-41-32; (g) Nb(Cl)/MCM-41-32; (h) Nb(O)/SiO_2-32.

(above 1000 K) the consumption of hydrogen starts at a lower temperature on the sample (a) than (b) indicating that the HT reduced niobium species is easier reducible when niobium-oxalate is used in the synthesis of NbMCM-41-32 sample (profile a). The material prepared from niobium ammonium-oxalate complex presents a very poor TPR profile (c). It is noteworthy that this sample exhibits an additional crystal phase observed in the XRD pattern [12], so its surface properties can be different from the ones of the other materials.

According to our earlier assumption [13], LT peaks origin from the reduction of extra framework niobium species, whereas HT signals are due to the reduction of framework niobium. In both cases more than one niobium species are detected during the reduction. In the HT region it is more visible when the sample is prepared from niobium-oxalate with Si/Nb = 16 (Fig. 1B, profile d). Various H_2-TPR peaks in HT region can be due either to the various steps of niobium reduction, or to the reduction of various Nb-species in the framework, or to the both cases. The border between the temperatures required for the reduction of extra framework and framework niobium species was estimated on the basis of H_2-TPR profiles of the samples prepared via the impregnation of siliceous MCM-41 with niobium salts (Fig. 1C). Both profiles exposed in part C exhibit one very sharp peak with the maximum at 920 and 943 K (for niobium chloride and oxalate used for the synthesis, respectively). This peak goes down to the base line at around 1000 K. The impregnated samples posses niobium species only in the extra framework position. There is not a significant difference in the intensity of both peaks presented in Fig. 1C. So, the nature of the niobium source does not effect the number of Nb and its reducibility in the impregnated molecular sieves. On the contrary, the peak due to the reduction of extra framework niobium species in the Nb(Cl)MCM-41-32 sample synthesised from $NbCl_5$ exhibits a much higher intensity than that one observed on the material synthesised from niobium-oxalate (Fig. 1A, profiles a and b). The higher amount of extra framework niobium species in Nb(Cl)MCM-41-32 results in the decrease of the pore volume as indicated in Table 1.

A small shoulders above 1000 K in Fig. 1C can be attributed to the reduction of a niobium species formed as a result of a kind of solid state interaction between the siliceous matrix (MCM-41) and extra framework niobium species.

The shape of the H_2-TPR profile does not depend on the amount of niobium-oxalate used for the impregnation of MCM-41. When Si/Nb = 16 ratio was applied, the TPR profile was the same as that of Nb(O)/MCM-41-32, the only difference was a lower temperature of the maximum reduction (915 K) and the higher intensity of the peak.

When silica is used as a support for niobium the H_2-TPR profile (Fig. 1D) differs from these performed in Fig. 1C. A broad peak with a maximum at ∼910 K covers almost the whole range of the temperatures and could be due to the reduction of various niobium species presenting various oxidative state or various surroundings.

As mentioned above, the high concentration of Nb in the Nb(O)MCM-41-16 sample allows distinguishing three H_2-TPR peaks in the HT region (Fig. 1B, d). They are also registered at a little lower temperature on the calcined sample (Fig. 1B, e).

3.2. FTIR study

Infrared spectroscopic study was applied for the characterisation of the catalyst surface. It allows the characterisation of the active centres which interact with NO molecules used as a probe for Lewis acid sites and also for electron donor centres [14,15]. Moreover, in the 850–1000 cm^{-1} range one can estimate the skeletal perturbations caused by the incorporation of cations other than Si (e.g. niobium) into the lattice [16,17], or by the skeletal interaction with the extra framework cation or adsorbed molecules [18–23].

Fig. 2 displays the FTIR spectra of the samples evacuated at 723 K (spectra A–C, a) and after NO adsorption at RT (spectra A–C, b). Evacuated NbMCM-41 mesoporous molecular sieves exhibit more than one IR bands in the region of 900–1000 cm^{-1}, whereas all materials show only one band (∼966 cm^{-1}) in this range if not evacuated (measured in the wafer with KBr — Fig. 3). Literature proposes various interpretations of the origin of the discussed bands [24–26]. However, it is now generally accepted that the band at ∼960 cm^{-1} is due to a Si–O vibrational mode perturbed by the presence of metal ions in a neighbouring position. Some authors use this band for evidence of the incorporation of metal into

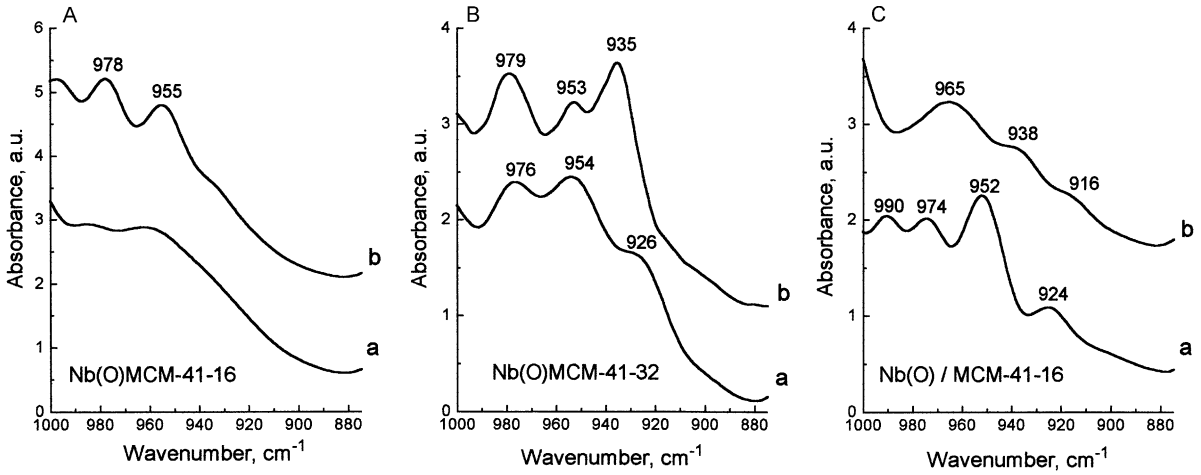

Fig. 2. FTIR spectra recorded in the vacuum IR cell: (a) samples after evacuation at 723 K, 3 h; (b) after NO adsorption at RT.

the siliceous framework (Si–O–T) [16,17]. Sarkany [21–23], Sobalik et al. [19,20] and Broclawik et al. [18] proposed the investigation of the properties of extra framework cations on the basis of IR bands in the 850–1000 cm^{-1} region. The interaction of cations with antisymmetric T–O–T vibration results in a shift of a band at 1020–1100 cm^{-1} (position characteristic of unperturbed vibration) to the "transmission window" situated between two strong bands of T–O–T antisymmetric and symmetric vibrations, i.e. in the range at 850–1000 cm^{-1}. The position of such a shifted band depends on the properties of cations and should be influenced by the cation position.

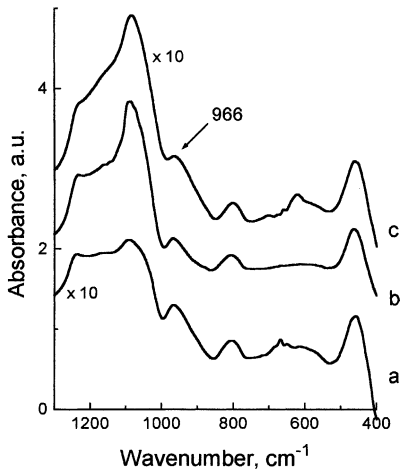

Fig. 3. FTIR spectra of (a) Nb(O)MCM-41-16; (b) Nb(O)MCM-41-32; (c) Nb(O)/MCM-41-16. The spectra correspond to a mixture of 1 mg of the sample into 200 mg of KBr.

The comparison of the spectra presented in Figs. 2 and 3 allows the observation of changes caused by the dehydroxylation of Nb(O)MCM-41-16 after evacuation at 723 K. The non-activated sample exhibits only one IR band at 966 cm^{-1} (Fig. 3), whereas the evacuated material presents two weak bands at ~955 and ~980 cm^{-1} (Fig. 2A). It is most probably due to the transformation of niobium species during the evacuation. According to our earlier statement [8], the dehydroxylation leads to the formation of two kinds of framework niobium, Nb^{+} and NbO^{-}. The influence of these two various Nb-species on Si–O vibration is different and therefore more than one IR band is registered. The band at ~955 cm^{-1} is asymmetric suggesting that it composes of two (or more) submaxima. They are evidenced in the Nb(O)MCM-41-32 sample (Fig. 2B, a). Apart from these two IR bands well visible in Nb(O)MCM-41-16 the third one at 926 cm^{-1} is registered on Nb(O)MCM-41-32. If the band at ~960 cm^{-1} origins from the interaction of NbOH in the framework (see hydroxylated sample, Eq. (1)) with T–O–T skeletal vibrations, the other two bands should be due to the dehydroxylated forms of niobium in the framework. They are well detected after NO adsorption. Fig. 4 displays the FTIR spectrum in the N–O stretching zone after NO adsorption on Nb(O)MCM-41-16. One can see two bands (1808 and 1629 cm^{-1}) ascribed to $Nb^{\delta+}NO^{\delta+}$ and $NbO^{\delta-}NO^{\delta-}$

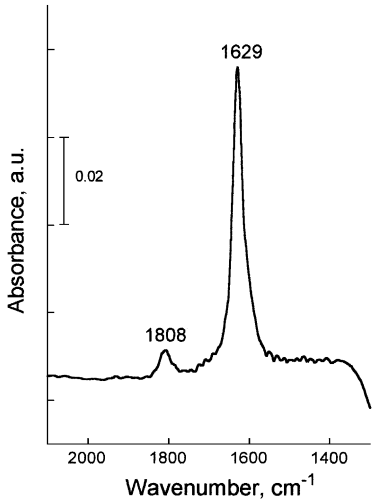

Fig. 4. FTIR spectrum, recorded in the vacuum IR cell, of Nb(O)MCM-41-16 after NO adsorption at RT.

complexes, respectively. They confirm the above discussed behaviour. The existence of the three bands in the region at 900–1000 cm^{-1} suggests that either the material is not fully dehydroxylated during the evacuation or that there are more than two types of niobium species. One cannot exclude that the third IR band is due to peroxide or superoxide species which gives rise to a band in the 1100–850 cm^{-1} zone.

In the case of the impregnated sample, Nb(O)/MCM-41-16, the IR spectrum (Fig. 2C, a) reveals more bands with various intensities, indicating various strength of the niobium species interaction with the skeletal vibrations. It is noteworthy that in this sample, niobium atoms occupies the extra framework position. The IR spectrum suggests the existence of various extra framework $Nb^{\delta+}$ and/or $NbO^{\delta+}$ cations interacting with various strength with skeletal T–O–T vibrations.

Significant differences in the IR spectra were found after NO adsorption at RT on the sample having Nb in the skeletal and the extra framework position (Nb(O)MCM-41-16 and Nb(O)MCM-41-32) and Nb only in the extra framework position (Nb(O)/MCM-41-16). In the first case, the NO adsorption results in the shift and the growth of the skeletal IR band intensities, whereas in the second one, the intensity decreases after the adsorption of NO. Broclawik et al. [18] showed that the adsorbed molecules cause the shift of the skeletal IR band position (in the region 930–975 cm^{-1}) and the change in their intensity in CuZSM-5 zeolites. This effect depends on the cation charge, its coordination and the nature of adsorbate. The strong influence was noted in [18], when NO was applied as an adsorbate. The changes registered in spectra b (Fig. 2A–C) after NO adsorption are in favour of the various localisation of Nb in the materials synthesised with niobium-oxalate and MCM-41 impregnated with this salt.

The NO interaction with the niobium-containing mesoporous molecular sieves of MCM-41 type could be detected in the FTIR spectra in the 1300–2200 cm^{-1} region (Fig. 5). The adsorption of NO at RT on the samples with $Si/Nb = 32$ prepared from various niobium sources leads to the formation of various IR bands (Fig. 5A–C). The nitrosyl species ($\nu(NO)^{\delta-}$) reported in many papers can be registered in 1800–1819 cm^{-1} region [27,28] or at 1740 cm^{-1} ($PtNO^{-}$) [29] or also at the other positions. The band at ~1806 cm^{-1} (Fig. 5B and C) can be assigned to NO adsorbed on the framework niobium cations whereas, that at ~1815 cm^{-1} to NO chemisorbed on the extra framework niobium cationic species (Fig. 5D). The origin of a band at 1630 cm^{-1} is not clear enough because in this region traces of water can also give rise to a band. We assigned the band in this region to the interaction of the framework NbO^{-} with NO (a kind of ONO^{-} species could be generated). In this paper, we would like to stress the formation of nitrate, nitrite and N_2O_3 species which can prove the oxidative properties of the surface. A broad band at ~1880 cm^{-1} develops under evacuation at 373 K showing that this species is slowly formed on the surface. This feature allowed us to attribute this band to stretching modes of N_2O_3 resulting from the NO molecule oxidation. A similar behaviour was found on Ce-, Sn-, and Sm-ZSM-5 zeolites [15]. Taking the assumption of Hadjiivanov et al. [30] such results could provide evidence for the existence of an active oxygen or oxygen ion due to some niobium form. The next oxidation step after N_2O_3 generation is the formation of nitrito and nitrato species observed in the region below 1600 cm^{-1}. The major evidence for their formation at RT is observed on Nb(O)MCM-41-32 sample (Fig. 5A). In the case of Nb(Cl)MCM-41-32 these species appear after heating at 373 K during evacuation (Fig. 5B, b). They are weakly visible at RT even using an expanded scale (Fig. 5B, a). The Nb(Oc)MCM-41-32

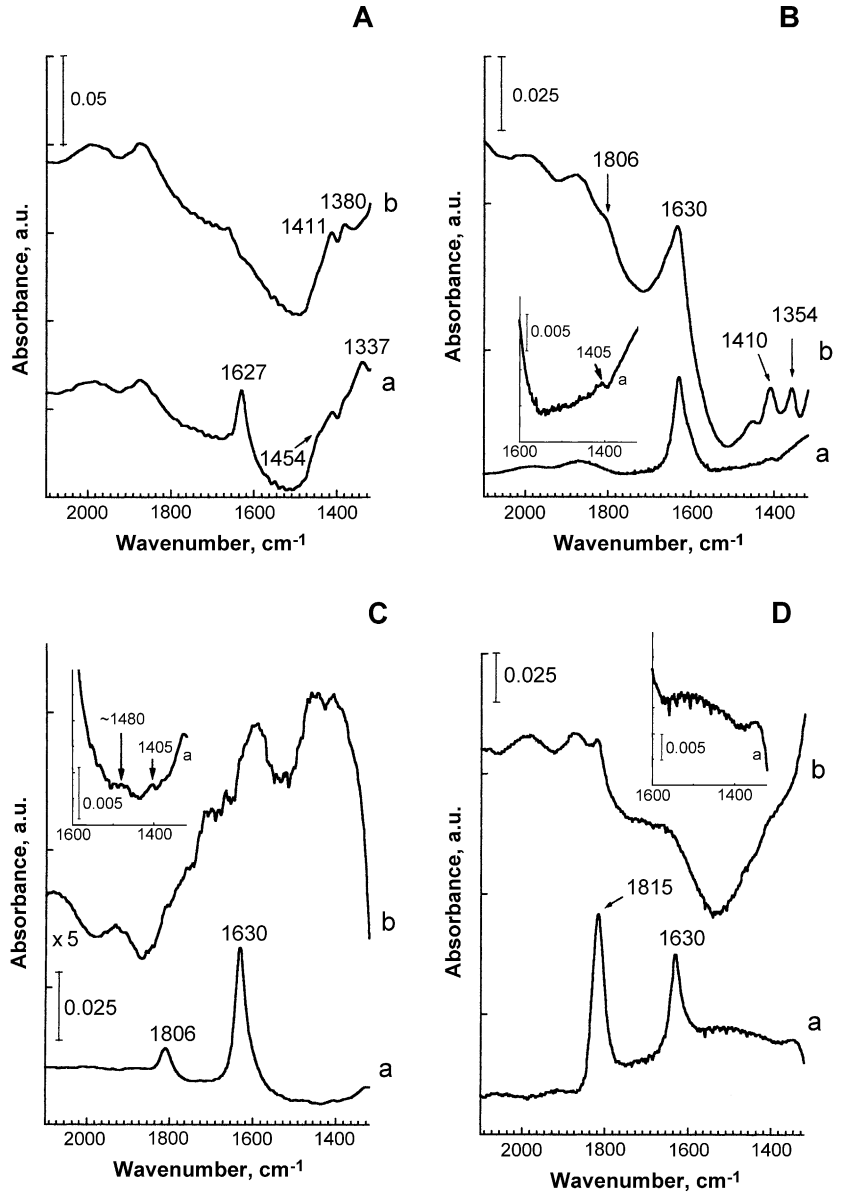

Fig. 5. FTIR spectra recorded in the vacuum IR cell: A — Nb(O)MCM-41-32; B — Nb(Cl)MCM-41-32; C — Nb(Oc)MCM-41-32; D — Nb(Cl) / MCM-41-32. (a) After NO adsorption at RT; (b) followed by evacuation at 373 K, 0.5 h.

sample exhibits a little more informative FTIR spectrum in the nitrito–nitrato region when it is plotted in the expanded absorbance scale (Fig. 5C).

Taking into account the formation of nitrito–nitrato species after NO adsorption at RT, the following order could be proposed:

$$\text{Nb(O)MCM-41-32} > \text{Nb(Oc)MCM-41-32} \geq \text{Nb(Cl)MCM-41-32}$$

The sample prepared via impregnation of MCM-41 with $NbCl_5$ (Fig. 5D) does not exhibit IR bands below 1600 cm^{-1} after NO adsorption at RT and evacuation

at 373 K. This sample presents a very intensive band at 1815 cm^{-1} which can be assigned to NO chemisorbed on an extra framework niobium species. The position of this band at a higher wavenumber (1815 cm^{-1}) than that registered on the material with niobium in the framework (∼1806 cm^{-1}) is caused by a weaker interaction of extra framework niobium cations with NO molecules (the IR band is closer to the band of NO gas phase (1880 cm^{-1})). It is noteworthy that the intensity of the band from the nitrosyl complex ($Nb^{\delta+}NO^{\delta-}$) is several times higher on the impregnated material than on the sample synthesised with niobium source even the Si/Nb ratio is the same (Fig. 5). It indicates that only a small part of niobium in the framework is accessible for the adsorbed molecules. It must be due to the wall thickness which was estimated [12] in the following order:

$$\text{Nb(Cl)MCM-41} > \text{Nb(O)MCM-41} > \text{Nb(Oc)MCM-41}$$

The smallest wall thickness in Nb(Oc)MCM-41 allows the exposition of the highest number of Nb-species for the interaction with the adsorbed molecules.

3.3. ESR study

Various paramagnetic species could exist on niobium-containing materials. If niobium is incorporated into the framework of MCM-41 mesoporous sieves one can expect the existence of paramagnetic Nb^{4+} exhibiting 10 hyperfine lines with $g \cong 1.89$ [16,31–33]. It could be more than 10 lines if a defect is located on Nb–O−Nb unit due to two Nb nuclei [16]. Moreover, oxygen radical species as well as a defect hole centre are possible to be formed during heating or irradiation. Previously [8], we have found the formation of oxygen radicals on the NbMCM-41-32 sample and we assigned them to the framework NbO^- formed as a result of the dehydroxylation (Eq. (1)). In this paper, we studied the influence of the Si/Nb ratio and Nb-source using for the synthesis on the ESR spectra. The results are shown in Fig. 6. Nb(O)MCM-41-32 sample evacuated at 723 K displays one sharp ESR signal ($g = 2.0025$) and a weak hyperfine structure (Fig. 6A, b). A sharp signal represents the defect centre which is a hole mainly localised on an oxygen atom and near a niobium atom. So, it would be assigned to Nb–O^- species [8,31,32]. However, one cannot exclude the participation of carbon radicals in the sharp ESR signal. The latest can be generated by heating of the residual template. A similar ESR spectrum was registered when the mesoporous sieve was produced from $NbCl_5$ (Fig. 6A, a).

The ESR spectrum of the Nb(O)MCM-41-16 sample (Si/Nb = 16, i.e. a higher concentration of Nb than in the samples characterised by Si/Nb = 32) (Fig. 6B, c) varies from those in Fig. 6A. It includes the signals with $g = 2.0010$; 2.0049 and 2.039 attributed on the basis of [34] to O_2^- radical, and

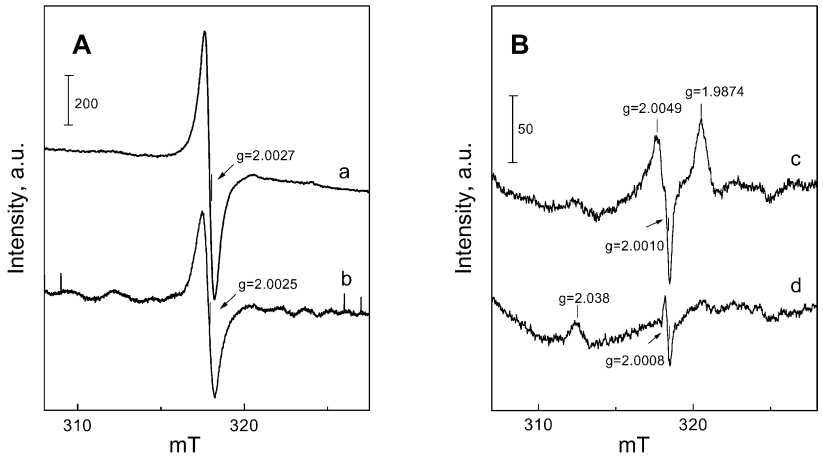

Fig. 6. ESR spectra recorded at 77 K. A — the samples evacuated at 723 K, 2 h; (a) Nb(Cl)MCM-41-32; (b) Nb(O)MCM-41-32; B — Nb(O)MCM-41-16; (c) evacuated at 723 K, 2 h; (d) after heating at 723 K, 0.5 h in the presence of oxygen.

another one with $g = 1.987$ assigned in the literature to the lattice defects [35] formed by the desorption or dissociation of oxygen (in [34] due to photo irradiation under vacuum). The decrease of the signal intensity with O_2 introduction and heating at 723 K (Fig. 6B, d) was caused by the readsorption of oxygen on the surface of the sample. The described behaviour can be explained by the high concentration of Nb–O^- species in Nb(O)MCM-41-16 which results in the easier release of oxygen than that from the sample with Si/Nb = 32. The $g_{zz} = 2.039$ of O_2^- radicals well correlates with that calculated by Che and Giamello [34] for O_2^- interacting with M^{4+} cations. Therefore, one can suppose that with a high Nb content (Si/Nb = 16), the partial reduction of Nb^{5+} to Nb^{4+} occurs under evacuation leading to the interaction with O_2^-.

3.4. Catalytic activity

The activity of Nb-containing catalysts in the oxidation processes was tested in the reaction of dibutyl sulphide with hydrogen peroxide. This process occurs according to the following reaction:

$$R_1\text{–}S\text{–}R_2 \xrightarrow[k_1]{H_2O_2} R_1\text{–}SO\text{–}R_2 \text{ (sulphoxide)}$$
$$\xrightarrow[k_2]{H_2O_2} R_1\text{–}SO_2\text{–}R_2 \text{ (sulphone)} \quad (3)$$

where $k_1 \gg k_2$.

Using the stoichiometric molar ratio of Bu_2S:$H_2O_2 = 1$ and a highly active catalyst one can obtain a high selectivity to sulphoxide due to $k_1 \gg k_2$. It is worthy to notice that the reaction proceeds also in the methanol solution without the catalyst. However, the process is slow and the conversion of Bu_2S slowly increases with time of stirring (Fig. 7a). In the homogeneous system, when Nb(V)-oxalate dissolved in methanol is applied as a catalyst, 90% of Bu_2S conversion is reached after 1 h of stirring (Fig. 7d), but the induction period for the growth of the activity is required. After c.a. 1 h, the selectivity to sulphoxide was 95%. The application of a heterogeneous catalyst, Nb(O)MCM-41-32 (Fig. 7e) allows reaching of 99% conversion of Bu_2S without the induction period and 98% selectivity to sulphoxide. The Nb(O)MCM-41-32 used was synthesised from Nb(V)-oxalate. The increase of niobium content

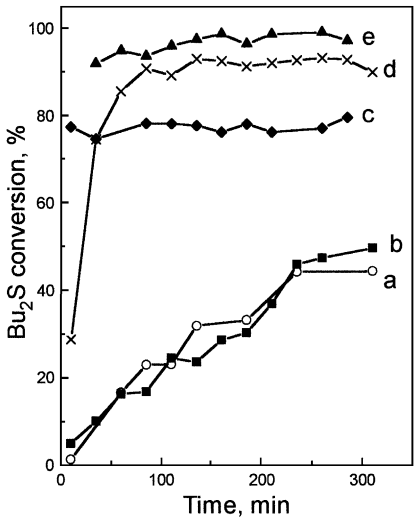

Fig. 7. Dibutyl sulphide conversion in the oxidation with H_2O_2 at 303 K: (a) without the catalyst; (b) Nb(O)/MCM-41-32; (c) Nb(O)-MCM-41-16; (d) in the methanol solution of niobium-oxalate; (e) Nb(O)MCM-41-32.

during the preparation (Si/Nb = 16) leads to the decrease of the activity (Fig. 7c), but the selectivity to sulphoxide is the same as on Nb(O)MCM-41-32. One should remind that the Nb(O)MCM-41-16 sample exhibits the secondary mesoporous system [12] and the lower pore size and pore volume than those of Nb(O)MCM-41-32. Therefore, the difference in the activity between both samples could be correlate with the diffusion effect. However, it is not the only feature affecting the activity because the oxidative properties of Nb(O)MCM-41-16 increases after heating the sample in the presence of oxygen at 723 K (Fig. 8). This behaviour should be correlated with the changes of paramagnetic properties (observed in the ESR spectra) after the calcination of the activated sample at 723 K in the presence of O_2.

The experiments carried out on the mesoporous materials (MCM-41) impregnated with Nb-oxalate (Si/Nb = 32 and 16) confirmed our earlier suggestion that only Nb incorporated to the lattice is responsible for the oxidation activity. Fig. 7b exhibits the conversion of Bu_2S on the impregnated material (Nb(O)/MCM-41-32). It is the same as in the reaction without the catalyst (Fig. 7a). However, when Nb-species formed after the impregnation are not strongly held on the surface of MCM-41 (e.g. when

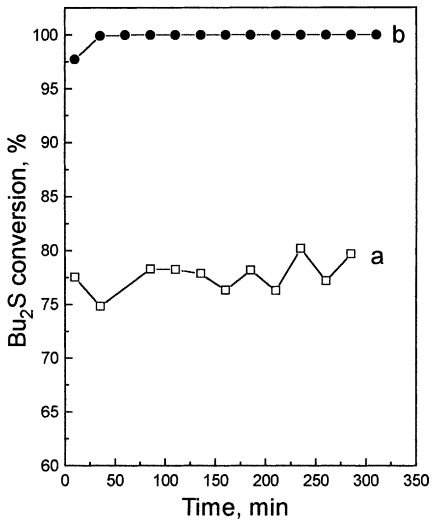

Fig. 8. Dibutyl sulphide conversion in the oxidation with H_2O_2 at 303 K on Nb(O)MCM-41-16 — the effect of calcination in the presence of oxygen. (a) The sample activated at 723 K in oven; (b) the sample calcined in the presence of oxygen at 723 K.

$NbCl_5$ is used for the impregnation), the leaching of Nb to the solution could occur and the reaction proceeds in the homogeneous phase.

The nature of Nb-source plays an important role in the oxidative properties of the material not only if a Nb-salt is applied for the impregnation, but also for the synthesis of niobio-siliceous mesoporous catalyst. Fig. 9 demonstrates this behaviour. The highest activity is observed when niobium(V)-oxalate is used for the synthesis (Fig. 9c) and the lowest in the case of $NbCl_5$ used as Nb-source (Fig. 9a). This indicates that oxalate ions play an important role in the generation of the centres active in the oxidation with H_2O_2.

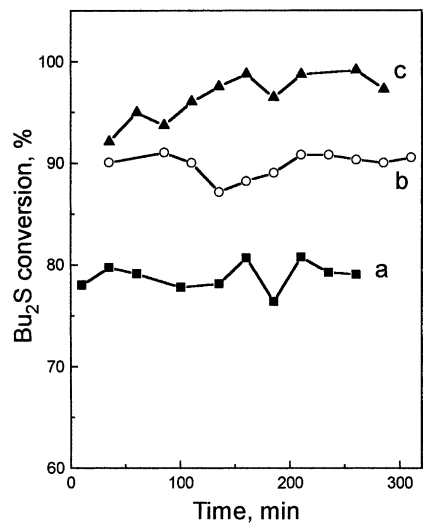

Fig. 9. Dibutyl sulphide conversion in the oxidation with H_2O_2 at 303 K — the effect of Nb-source used in the synthesis of the catalyst. (a) Nb(Cl)MCM-41-32; (b) Nb(Oc)MCM-41-32; (c) Nb(O)MCM-41-32.

When the cation exchange (Ni, Cu) in Nb(O)MCM-41-32 material was carried out, the extra lattice nickel or copper cations interact with the framework $Nb–O^-$ species resulting in the deactivation of the catalyst in the oxidation of Bu_2S.

4. Discussion

The catalytic sulphoxidation of thioethers with hydrogen peroxide requires the electrophilic properties of the catalyst necessary to activate the oxidising agent. Moreau and coworkers [36,37] described the high activity of TS-1 and Ti-beta catalysts in this process. They have found that the oxidation of thioethers with H_2O_2 involves the nucleophilic attack of the sulphur atom on the oxygen atom of a hydroperoxo-Ti complex coordinated by a molecule of the solvent. The structure of NbMCM-41 materials, which were discovered as highly active catalysts in the oxidation of thioethers with H_2O_2 [8,38], differs from those of TS-1 and Ti-beta mainly due to the various oxidation state of Nb(V) and Ti(IV) incorporated into the framework. The characterisation of the Nb-containing mesoporous catalysts carried out in this work allows us to define some features responsible for the activity of NbMCM-41 materials in the thioethers oxidation.

FTIR study in the skeletal range and H_2-TPR measurements helped to localise the position of Nb (in the framework or in the extra framework sites). The Si–O–Si vibrations observed in the 1020–1100 cm^{-1} range are perturbed in the various manner depending on the location of the niobium cations (framework or extra framework) and their interaction with Si–O–Si vibrational mode [18–23]. The appearance of two IR bands in the transmission window (850–1000 cm^{-1}) on the Nb(O)MCM-41-16 sample evacuated at 723 K indicates the presence of two various Nb-species interacting with T–O–T vibration. We propose that they are NbO^- and Nb^+ in the framework which shift

a band (1020–1100 cm^{-1}) of a skeletal vibration of Si–O with various $\Delta\nu$ depending on the strength of the interaction, determined by the ion charge. The discussed Nb-species origin from the framework, because the chemisorbed molecules (NO) raise the intensity of the perturbed vibrational bands. It can occur only when niobium is localised in the framework (Si–O–Nb), because its interaction with NO molecule lengthens Nb–O bond and shortens Si–O bond causing the increase of the perturbation effect. This effect runs in an opposite way if Nb is localised outside the framework (as in the impregnated samples). This is because the strong interaction of Nb-extra framework species with the adsorbate (NO) weakness its interaction with the skeletal T–O–T vibrations reducing the intensity of the perturbed IR bands.

The existence of various types of framework and extra framework Nb-species was confirmed by the results of the H_2-TPR studies. The samples prepared from Si- and Nb-sources exhibit both extra framework and framework positions, both occupied by various Nb-species, which present various possibility of the reduction. Framework Nb-species are reduced at a higher temperature than that of the reduction of the extra framework niobium cations. The reduction temperature depends on a kind of Nb-salts used for the synthesis of NbMCM-41 materials. It is lower for the framework Nb, if the sample is prepared from niobium-oxalate than when $NbCl_5$ is used for the synthesis of mesoporous sieves. The role of the nature of an anion in the Nb-source on the properties of the final material is proved by the H_2-TPR experiments.

A nature of Nb-source influences also the oxidising properties of NbMCM-41 sieves in relation to the adsorbed molecules, e.g. NO. Fig. 5 displays the formation of nitrito–nitrato species (IR bands below 1600 cm^{-1}) depending on the Nb-source used in the synthesis and allow the formulation of the following order:

$$\text{Nb(O)MCM-41-32} > \text{Nb(Oc)MCM-41-32} > \text{Nb(Cl)MCM-41-32}$$

This order is in the agreement with the activity in the *n*-dibutyl sulphide oxidation (Fig. 9) and also with the physical parameters of the materials; namely, a pore size and a pore volume. It is noteworthy that the oxalate ion (in both niobium-oxalate and niobium ammonium-oxalate complex) could play a role in the formation of the active centres during the synthesis of NbMCM-41.

The activity of Nb-containing mesoporous molecular sieves requires the presence of $Nb–O^-$ in the framework. The siliceous MCM-41 impregnated with niobium-oxalate is inactive in the oxidation of Bu_2S. The incorporation of Ni or Cu cations via a cation exchange procedure to Nb(O)MCM-41-32 material causes the deactivation of the catalyst in relation to the oxidation of Bu_2S. Metal cations in the extra framework position blockage the $Nb–O^-$ framework species. The formation of this species during a temperature activation depends on the concentration of Nb in the framework. If this concentration is high (Si/Nb = 16), the HT treatment (723 K) of the sample causes the release of oxygen from neighbouring $Nb–O^-$ species leading to the defect formation (registered in the ESR spectra — Fig. 6, $g \cong 1.89$). It is a reason for a lower Nb(O)MCM-41-16 activity in the oxidation of Bu_2S than that of the Nb(O)MCM-41-32 sample. When the defected material is calcined in the presence of oxygen at 723 K, the activity of Nb(O)MCM-41-16 significantly increases (Fig. 8). The chemisorbed oxygen rebuilt the $Nb–O^-$ framework species active in the $Bu_2S + H_2O_2$ reaction.

The concentration of niobium in the framework affects the reduction of Nb as proved in the ESR study. The higher Nb content (Si/Nb = 16) the easier reduction of niobium during the activation under vacuum or in a He flow.

5. Conclusions

- The H_2-TPR study and FTIR measurements in the transmission window of the skeletal range (850–1000 cm^{-1}) with NO as a probe molecule allow the distinguish between Nb in the framework and in the extra framework positions in the mesoporous molecular sieves of MCM-41 type.
- The activity of Nb-containing mesoporous molecular sieves in the oxidation of thioethers with H_2O_2 requires the presence of $Nb–O^-$ species in the framework.
- Extra framework cationic niobium-species in MCM-41-16 sieves are not active in the Bu_2S

oxidation with H_2O_2, unless they are leached to the solution during the reaction.

- Oxalate ions present in the Nb-source used in the synthesis of mesoporous sieves seems to influence the formation of the oxidative centres in NbMCM-41 materials.
- A HT activation of NbMCM-41 materials with a high niobium content (Si/Nb = 16) leads to the disappearance of a part of Nb–O^- species due to the release of oxygen and the formation of the defects. This process is reversible and after oxygen treatment at a HT the oxidative activity is restored.
- There is a good correlation between the activity of the catalysts in the oxidation of Bu_2S with H_2O_2 and the formation of nitrito–nitrato species after the adsorption of NO on the materials (detected by a FTIR technique).

Acknowledgements

This work was partially supported by KBN (Polish State Committee for Scientific Research), Grant No. 3 TO9A 10219. Maria Ziolek is grateful for an opportunity to work with Dr. Jean-Claude Lavalley, a great scientist, and a friend. During the long-term collaboration, his indispensable advice and support for Polish–French cooperation among under-graduate and graduate students proved to be of great value for scientific research in the field of FTIR spectroscopy.

References

[1] R.A. Sheldon, J.W.C.E. Arends, H.E.B. Lampers, Catal. Today 41 (1998) 387.
[2] R.A. Sheldon, Chemtech 21 (1991) 566.
[3] R.A. Sheldon, J. Mol. Catal. A 107 (1996) 75.
[4] J.W.C.E. Arends, R.A. Sheldon, M. Wallan, U. Schuchardt, Angew. Chem. Int. Ed. Engl. 36 (1997) 1144.
[5] M. Ziolek, I. Nowak, Zeolites 18 (1997) 356.
[6] M. Ziolek, I. Nowak, J.C. Lavalley, Catal. Lett. 45 (1997) 259.
[7] L. Zhang, J.Y. Ying, AIChEJ. 43 (1997) 2793.
[8] M. Ziolek, I. Sobczak, I. Nowak, P. Decyk, A. Lewandowska, J. Kujawa, Micropor. Mesopor. Mater. 35/36 (2000) 195.
[9] M. Ziolek, I. Nowak, I. Sobczak, A. Lewandowska, P. Decyk, J. Kujawa, Stud. Surf. Sci. Catal. 129 (2000) 813.
[10] P.A. Jacobs, Plenary lecture, in: Proceedings of the First International FEZA Conference, Eger, Hungary, September 1–4, 1999.
[11] S.B. Park, P.M. Wood, B.C. Gilbert, A.C. Whitwood, J. Chem. Soc., Perk. Trans. 2 (1999) 923.
[12] I. Nowak, submitted for publication.
[13] I. Sobczak, M. Ziolek, unpublished data.
[14] J.L.G. Fierro, Stud. Surf. Sci. Catal. B 57 (1990) 67.
[15] V.I. Parvulescu, P. Grange, B. Delmon, J. Phys. Chem. B 101 (1997) 6933.
[16] A.M. Prakash, L. Kevan, J. Am. Chem. Soc. 120 (1998) 13148.
[17] B. Notari, Adv. Catal. 41 (1996) 253.
[18] E. Broclawik, J. Datka, B. Gil, P. Kozyra, Phys. Chem. Chem. Phys. 2 (2000) 401.
[19] Z. Sobalik, Z. Tvaruzkova, B. Wichterlova, J. Phys. Chem. 102 (1998) 1077.
[20] Z. Sobalik, J. Dedecek, I. Ikonnikov, B. Wichterlova, Micropor. Mesopor. Mater. 21 (1998) 525.
[21] J. Sarkany, J. Mol. Struct. 410–411 (1997) 95.
[22] J. Sarkany, J. Mol. Struct. 410–411 (1997) 137.
[23] J. Sarkany, J. Mol. Struct. 410–411 (1997) 145.
[24] H.Y. Chen, L. Chen, J. Lin, K.L. Tan, J. Li, Inorg. Chem. 36 (1997) 1417.
[25] R. Kumar Rana, B. Viswanathan, Catal. Lett. 52 (1998) 25.
[26] El-M. El-Malki, R.A. van Santen, W.M.H. Sachtler, J. Phys. Chem. B 103 (1999) 4611.
[27] T. Cheung, S.K. Bhargava, M. Hobday, K. Foger, J. Catal. 158 (1996) 301.
[28] D.B. Akolekar, S.K. Bhargava, K. Foger, J. Chem. Soc., Faraday Trans. 94 (1998) 155.
[29] D.K. Captain, M.D. Amiridis, J. Catal. 184 (1999) 377.
[30] K. Hadjiivanov, K. Klissurski, D. Ramis, G. Busca, Appl. Catal. B 7 (1996) 251.
[31] D. de A.B. Filho, D.W. Franco, P.P.A. Filho, O.L. Alves, J. Mater. Sci. 33 (1998) 2607.
[32] Y.M. Kim, D.E. Reardon, P.J. Bray, J. Chem. Phys. 48 (1968) 3396.
[33] M. Sugantha, G.V. Subbo Rao, J. Solid State Chem. 111 (1994) 33.
[34] M. Che, E. Giamello, Stud. Surf. Sci. Catal. B 57 (1990) 265.
[35] H. Kokusen, S. Matsuhara, Y. Nishino, S. Hasegawa, K. Kubono, Catal. Today 28 (1996) 191.
[36] V. Hulea, P. Moreau, F. Di Renzo, J. Mol. Catal. A 111 (1996) 325.
[37] V. Hulea, P. Moreau, J. Mol. Catal. A 111 (1996) 499.
[38] M. Ziolek, I. Nowak, H. Poltorak, A. Lewandowska, I. Sobczak, Stud. Surf. Sci. Catal. 125 (1999) 691.